Tunable Subterahertz Wave Generation Based on Photonic Frequency Sextupling Using a Polarization Modulator and a Wavelength-Fixed Notch Filter

Shilong Pan, *Member, IEEE*, and Jianping Yao, *Senior Member, IEEE*

***Abstract*—Optical frequency multiplication based on electrooptical modulation is an effective way to generate high-spectral-purity and frequency-tunable subterahertz waves. The previously demonstrated frequency-doubling and quadrupling techniques based on a Mach–Zehnder modulator have a low multiplication factor and suffer from bias drift problem and residual chirp. In this paper, a novel approach to achieving frequency sextupling using a polarization modulator and a wavelength-fixed optical notch filter is proposed and experimentally demonstrated. The method is free from bias drift problem and residual chirp, which can be used to generate high-spectral-purity subterahertz wave signals using relatively low-frequency electrical and optical devices. By using a narrow-bandwidth fiber Bragg grating as a wavelength-fixed optical notch filter, a high-spectral-purity microwave signal tunable from 18 to 27.6 GHz is generated when a microwave drive signal from 3 to 4.6 GHz is applied to the polarization modulator. The phase noise of the generated signal is measured as low as −107.57 dBc/Hz at a 10-kHz offset frequency. By replacing the narrow-bandwidth notch filter by an optical interleaver, a subterahertz wave tunable from 66 to 114 GHz is generated when the drive signal is tuned from 11 to 19 GHz. The distribution of the generated signal over optical fiber is investigated. The results show that the quality of the distributed subterahertz wave signal is maintained after transmission over a 40-km standard single-mode fiber.**

***Index Terms*—Microwave photonics, polarization modulator, terahertz generation.**

I. Introduction

MILLIMETER waves and terahertz waves, covering a frequency range from 30 GHz to 10 THz, are very attractive for applications in spectroscopic sensing [1]–[3] and ultrabroadband wireless communications [4], [5]. A spectroscopic system using frequency-tunable continuous-wave (CW) terahertz sources is found to have a higher signal-to-noise ratio and spectral resolution as compared with a pulsed-terahertz-based system [6]. To generate high-frequency and frequency-tunable CW terahertz waves, the most promising method is to heterodyne two light waves at a photomixer or photodetector with a wavelength difference that falls in the terahertz range [7]. To generate a terahertz wave with high spectral purity, the two optical waves applied to the photomixer or photodetector for heterodyne must be phase correlated.

A simple and cost-effective way to produce two optical waves is to employ a dual-wavelength single-longitudinal-mode laser source [8]–[12] or two free-running semiconductor lasers [13]. However, the generated terahertz wave has a large phase noise. To increase the phase correlation, an optical phase-locked loop (PLL) can be employed [14]–[16]. However, expensive electrical devices operating at high frequency are required to extract the phase information from the high-frequency beat signal, which makes the system complicated and costly.

Two phase-correlated optical waves can also be generated by optical frequency multiplication of a low-frequency microwave reference signal, in which a single laser source is needed. Since the frequency multiplication is a nonlinear process, a nonlinear device must be used, which can be a highly nonlinear fiber (HNLF) or a semiconductor optical amplifier to achieve four-wave mixing (FWM) [17]–[19] leading to the generation of a frequency-tripled electrical signal. The major problem associated with the FWM effects is its ultralow conversion efficiency. Frequency multiplication can also be achieved using an optical modulator [20]–[29]. Compared with the use of a nonlinear optical device, the techniques using an optical modulator are of greater interest thanks to the simplicity, tunability, higher nonlinear efficiency, and better stability. For instance, an optical frequency comb consisting of multiple optical spectral lines was generated by phase modulation of an optical carrier at an electrooptic phase modulator [20]–[22]. With two narrowband optical filters to select two of these spectral lines, two phase-correlated light waves with a frequency spacing tunable from the reference frequency to N (N can be larger than 50) times the reference frequency are obtained, which can be used to generate a low phase noise and continuously frequency-tunable subterahertz-wave signal. However, the two optical filters must be tunable to ensure the frequency tunability.

To generate a frequency-tunable millimeter-wave signal without using tunable optical filters, Qi *et al.* proposed using a Mach–Zehnder modulator (MZM) that was biased at the maximum transmission point to eliminate the odd-order sidebands [23]. By using a wavelength-fixed optical notch filter to remove the optical carrier, a microwave or millimeter-wave signal with a frequency that is four times the frequency of the microwave drive signal was generated. The frequency tunability was achieved by simply tuning the frequency of the microwave

Manuscript received October 01, 2009; revised February 08, 2010; accepted March 11, 2010. Date of publication June 28, 2010; date of current version July 14, 2010. This work was supported by the Natural Sciences and Engineering Research Council of Canada (NSERC).

The authors are with the Microwave Photonics Research Laboratory, School of Information Technology and Engineering, University of Ottawa, Ottawa, ON, Canada K1N 6N5 (e-mail: jpyao@site.uOttawa.ca).

Color versions of one or more figures in this paper are available online at http://ieeexplore.ieee.org.

Digital Object Identifier 10.1109/TMTT.2010.2050182

drive signal. Other configurations that can be used to achieve frequency quadrupling include the use of two cascaded $LiNbO_3$ MZMs that are biased at the minimum transmission points [24] and the use of a specially designed $LiNbO_3$ MZM consisting of three sub-MZMs which are also biased at the minimum transmission points [25].

A disadvantage of the approaches in [23]–[25] is the bias drift of the MZMs. The bias drift of the MZMs which are biased at the minimum or maximum transmission points would significantly affect the spectral purity of the generated signal. Based on [30], a $\sim$2% drift of the dc bias can make the suppression ratio of the first-order sideband to the carrier drop by $\sim$30 dB. More important, the bias drift is intrinsic for a MZM; the $\sim$2% drift of the dc bias may happen in several seconds, which makes the system unstable or a sophisticated control circuit is needed to stabilize the operation. In addition, it is difficult to achieve an ideal 50/50 splitting ratio in the Y-splitter of a MZM due to the fabrication tolerances, which would result in a residual chirp, leading to a poor suppression of the odd-order or even-order sidebands even when the bias of the MZM is carefully adjusted, which would degrade the spectral purity of the generated electrical signals. The situation would be more severe when the frequency of the drive signal is high, making the scheme only applicable for the generation of an electrical signal at a few tens of gigahertz.

To avoid the above problems, an optical phase modulator may be used to replace the MZM [26], [27]. Again, by using a wavelength-fixed optical filter to remove the optical carrier, a frequency-doubled or quadrupled microwave signal could be generated. The major limitation of the approach using a phase modulator is that all sidebands are generated; therefore, if only the optical carrier is removed using a wavelength-fixed optical filter, at the output of the photodetector, an electrical signal consisting of a frequency-doubled and quadrupled frequency components will be generated. Recently, we have proposed a photonic microwave quadrupler using a polarization modulator [28]. Compared with the approaches in [23]–[27], the method is more attractive due to the higher spectral purity of the generated signal, better simplicity, and improved operation stability.

In [23]–[28], the frequency multiplication factor is only four. To generate an electrical signal with a frequency up to the subterahertz range using relatively low-frequency electrical and electrooptic devices, a higher frequency multiplication factor is highly desirable.

In this paper, we propose and experimentally demonstrate a novel method to generate a high-spectral-purity and frequency-tunable subterahertz-wave signal using a photonic frequency sextupler. The proposed frequency sextupler consists of a polarization modulator and a wavelength-fixed optical notch filter. The key significance of using a polarization modulator is that the modulator is not biased, which eliminates the bias drift problem. In addition, the residual chirp can be adjusted to zero by tuning a polarization controller (PC) placed before the polarization modulator. A theoretical analysis on the frequency tuning range and harmonic suppression ratio under different phase-modulation indices and filter attenuations is performed, and an experiment to verify the analysis is carried out. A high-spectral-purity microwave signal tunable from 18 to 27.6 GHz is generated when a microwave drive signal from 3 to 4.6 GHz is applied to the polarization modulator. The phase noise of the generated signal is measured as low as -107.57 dBc/Hz at a 10-kHz offset frequency. The generation of a stable electrical signal tunable from 66 to 114 GHz is also demonstrated by tuning the microwave drive signal from 11 to 19 GHz. The distribution of the generated subterahertz wave signal over optical fiber is investigated.

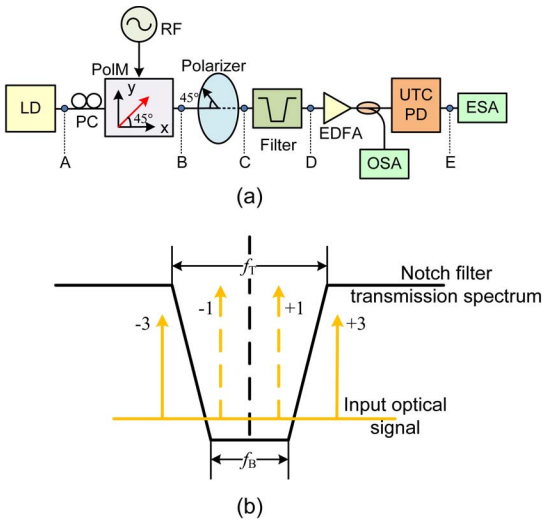

Fig. 1. (a) Block schematic diagram of the millimeter wave generation system. (b) Transmission spectrum of a wavelength-fixed notch filter showing a frequency tuning range from f_T to 3 f_B. LD: laser diode; RF: radio frequency; PC: polarization controller; PolM: polarization modulator; UTC-PD: unitraveling-carrier photodetector; EDFA: erbium-doped fiber amplifier; ESA: electrical spectrum analyzer; OSA: optical spectrum analyzer.

II. Analysis

A. System Architecture

The schematic of the proposed frequency sextupler is shown in Fig. 1(a). The system consists of a laser diode (LD), a polarization modulator, an optical polarizer, a wavelength-fixed optical notch filter, an erbium-doped fiber amplifier (EDFA), and a unitraveling-carrier photodetector (UTC-PD). A CW light wave from the LD is sent to the polarization modulator, which is driven by a microwave signal with a frequency of f_m. The polarization modulator is a special phase modulator that can support both TE and TM modes with opposite phase-modulation indices [31]. When a linearly polarized incident light wave oriented with an angle of 45° to one principal axis of the polarization modulator is sent to the polarization modulator, a pair of complementary phase-modulated signals is generated along the two principal axes of the polarization modulator. Applying the two signals to the optical polarizer with its polarization axis aligned with an angle of 45° with respect to one principal axis of the polarization modulator, the phase-modulated signals will be combined to generate an intensity-modulated signal with the even-order sidebands including the optical carrier suppressed. A wavelength-fixed notch filter is then used to filter out the two first-order sidebands. As a result, two phase-correlated optical waves with a wavelength spacing of 6 f_m are generated. By beating the two optical waves at the photodetector, a millimeter-wave signal at six times the frequency of the electrical

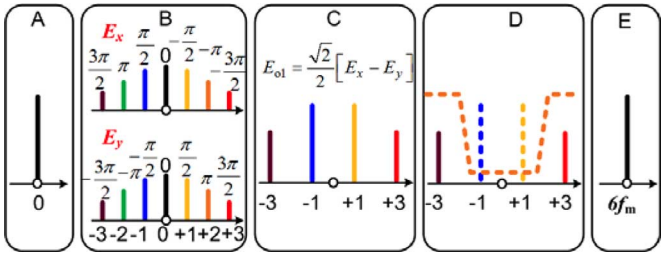

Fig. 2. Illustration of the operation principle. A, B, C, D: the optical spectra at different locations in the system shown in Fig. 1(a); E: the electrical spectrum at E.

drive signal is generated. Because no bias is needed for the polarization modulator, the system is free from bias drift, and a stable operation is guaranteed. In addition, the frequency of the generated millimeter-wave signal can be tuned by simply tuning the frequency of the electrical drive signal.

B. Frequency-Sextupled Millimeter-Wave Signal Generation

Fig. 2 shows the spectra at different locations in the system shown in Fig. 1(a). The CW light wave from the laser diode that is oriented with an angle of 45° to one principal axis of the polarization modulator is phase modulated in the polarization modulator along the x- and y-directions by a microwave drive signal with an angular frequency of $\omega_{\rm m}(\omega_{\rm m}=2\pi f_{\rm m})$. The normalized optical field at the output of the polarization modulator along the x- and y-directions can be expressed as

$$\begin{bmatrix} E_{\rm x}(t) \\ E_{\rm y}(t) \end{bmatrix} = \frac{\sqrt{2}}{2}\begin{bmatrix} \exp\left[j\omega_c t + j\beta\sin\omega_{\rm m}t\right] \\ \exp\left[j\omega_c t - j\beta\sin\omega_{\rm m}t\right] \end{bmatrix} \tag{1}$$

where $\omega_{\rm c}$ is the angular frequency of the optical carrier and β is the phase-modulation index of the polarization modulator. Applying the two signals to a polarizer with its principal axis aligned with an angle of 45° to one principal axis of the polarization modulator as shown in Fig. 1(a), we obtain

$$\begin{aligned} E_{\rm o1}(t) &= \frac{\sqrt{2}}{2}[E_{\rm x}-E_{\rm y}] \\ &= \sin(\beta\sin\omega_{\rm m}t)\cdot\exp(j\omega_{\rm c}t) \\ &= 2\exp(j\omega_{\rm c}t)\cdot\sum_{n=1}^{\infty}J_{2n-1}(\beta)\sin[(2n-1)\omega_{\rm m}t] \end{aligned} \tag{2}$$

where J_{2n-1} is the $(2n-1)$th-order Bessel function of the first kind.

As can be seen only odd-order sidebands are present at the output of the polarizer. The amplitude distribution of the sidebands is a function of β governed by the Bessel function. To generate optical sidebands up to the third order, β should be properly controlled to be around $\pi/2$. When this optical signal is fed to a photodetector, a frequency-doubled electrical signal and a frequency-sextupled electrical signal will be generated. To generate a frequency-sextupled electrical signal only, a wavelength-fixed optical notch filter to remove the two first-order sidebands is needed. The transmission spectrum of a wavelength-fixed optical notch filter is shown in Fig. 1(b). After the optical filtering, the optical signal can then be expressed as

$$E_{\rm o}(t) \approx 2\exp(j\omega_{\rm c}t)\cdot J_3(\beta)\cdot\sin(3\omega_{\rm m}t). \tag{3}$$

As a result, two optical sidebands separated by six times the frequency of the microwave drive signal are generated. Since the two sidebands originate from the same optical and microwave sources, a good phase correlation is maintained. Beating the two wavelengths at a photodetector, a high-spectral-purity frequency-sextupled microwave signal is generated. The photocurrent of the generated microwave signal is

$$I(t) \approx -2RJ_3^2(\beta)\cos(6\omega_{\rm m}t) \tag{4}$$

where R is the responsibility of the photodetector.

C. Frequency Tunability

In the system shown in Fig. 1(a), an optical notch filter is used to remove the two first-order sidebands. Ideally, the notch filter should have zero transmission over a certain range of frequency and 100% transmission elsewhere. This would support the frequency-sextupled microwave generator to be tunable in a certain frequency range, in which the two first-order sidebands are sufficiently suppressed by the optical notch filter while the two third-order sidebands are not attenuated.

We assume that the optical notch filter has an isosceles-trapezoid-shaped transmission spectral profile with the spectral width defined by the lower and upper limits denoted by $f_{\rm T}$ and $f_{\rm B}$, respectively, as shown in Fig. 1(b). The assumption is justified in practice since the two slopes of the notch filter will not be used. Since the two first-order sidebands should be removed, the two sidebands must be located in the stopband of the notch filter, which gives a maximum spacing between the two first-order sidebands of $f_{\rm B}$. To ensure that the two third-order sidebands are not attenuated, the spacing of the two third-order sidebands must be larger than $f_{\rm T}$. As a result, the frequency of the proposed millimeter wave generator can be tuned in the range

$$f_{\rm T} \le f \le 3f_{\rm B}. \tag{5}$$

It should be noted that the optical carrier is always located at the center of the stopband. Therefore, the optical notch filter does not need to be tunable. This feature ensures that the proposed approach can generate a frequency-tunable millimeter wave signal by simply tuning the frequency of the microwave drive signal without the need to tune the optical filter.

The highest frequency that can be generated by the system is limited by the bandwidth of the photodetector and the polarization modulator. So far, a photodetector based on the unitraveling carrier structure allows an effective detection of an optical microwave signal up to 914 GHz [32]. Meanwhile, a polarization modulator with a bandwidth in excess of 50 GHz has been developed [33]. Therefore, the maximum frequency of the generated millimeter-wave signal can be as high as 300 GHz, limited by the polarization modulator.

D. Electrical Harmonic Suppression

Assume that all of the even-order optical sidebands can be completely suppressed by carefully adjusting the polarization

direction of the polarizer. Assume also that the two first sidebands are attenuated with an attenuation of α dB by the optical notch filter. Based on the above assumptions, from (2), the optical signal at the output of the optical notch filter can be rewritten as

$$E_{\rm o}(t) = 2k\exp(j\omega_{\rm c}t)J_1(\beta)\sin\omega_{\rm m}t + 2\exp(j\omega_{\rm c}t)\sum_{n=2}^{\infty} J_{2n-1}(\beta)\sin[(2n-1)\omega_{\rm m}t] \quad (6)$$

where k is related to α by $\alpha = -20\log_{10} k$.

For practical applications, the phase-modulation index β is usually less than π, due to the limited microwave power applied to the polarization modulator. For $0 \le \beta \le \pi$, the Bessel function J_{2n-1} for $n \ge 2$ are all monotonically increasing with respect to β and monotonically decreasing with respect to the order of Bessel function n, and $J_3(\pi) = 0.33346$, $J_5(\pi) = 0.05214$, and $J_7(\pi) = 0.00342$. Therefore, it is reasonable to ignore the optical sidebands with orders higher than 5 in our analysis. Thus, (6) can be simplified to

$$\begin{aligned} E_{\rm o}(t) = {} & 2k\exp(j\omega_{\rm c}t)J_1(\beta)\sin\omega_{\rm m}t \\ & + 2\exp(j\omega_{\rm c}t)J_3(\beta)\sin 3\omega_{\rm m}t \\ & + 2\exp(j\omega_{\rm c}t)J_5(\beta)\sin 5\omega_{\rm m}t. \end{aligned} \quad (7)$$

Applying this optical signal to a photodetector, an electrical signal containing different orders of harmonics will be generated as

$$I(t) \propto -\sqrt{I_2}\cos 2\omega_{\rm m}t - \sqrt{I_4}\cos 4\omega_{\rm m}t - \sqrt{I_6}\cos 6\omega_{\rm m}t - \sqrt{I_8}\cos 8\omega_{\rm m}t - \sqrt{I_{10}}\cos 10\omega_{\rm m}t \quad (8)$$

where I_2, I_4, I_6, I_8 and I_{10} are the powers of the second-, fourth-, sixth-, eighth-, and tenth-order electrical harmonics, given by

$$I_2(t) = \left[k^2J_1^2(\beta) - 2kJ_1(\beta)J_3(\beta) - 2J_3(\beta)J_5(\beta)\right]^2 \quad (9)$$

$$I_4(t) = \left[2kJ_1(\beta)J_3(\beta) - 2kJ_1(\beta)J_5(\beta)\right]^2 \quad (10)$$

$$I_6(t) = \left[J_3^2(\beta) + 2kJ_1(\beta)J_5(\beta)\right]^2 \quad (11)$$

$$I_8(t) = \left[2J_3(\beta)J_5(\beta)\right]^2 \quad (12)$$

$$I_{10}(t) = J_5^4(\beta). \quad (13)$$

The power of the sixth-order harmonic I_6 and the harmonic suppression ratios of $I_6/I_2, I_6/I_4, I_6/I_8$ and I_6/I_{10} are plotted in Fig. 3. From Fig. 3(a), we can see that the power I_6 is monotonically increasing for $0 \le \beta \le \pi$. Fig. 3(b) is calculated when $\alpha = 60$ dB. The harmonic suppression ratios of I_6/I_8 and I_6/I_{10} are monotonically decreasing and I_6/I_4 is monotonically increasing for $0 \le \beta \le \pi$. The ratio I_6/I_2 is generally less than the ratios $I_6/I_4, I_6/I_8$ and I_6/I_{10} with a peak value of 23.5 dB at $\beta = 0.37\pi$.

To evaluate the harmonic suppression performance of the generated electrical signals, we define a new term called global suppression ratio $S_{\rm R}$. For a given β, the global suppression ratio is given by

$$S_{\rm R} = \min\left\{\frac{I_6}{I_2}, \frac{I_6}{I_4}, \frac{I_6}{I_8}, \frac{I_6}{I_{10}}\right\}. \quad (14)$$

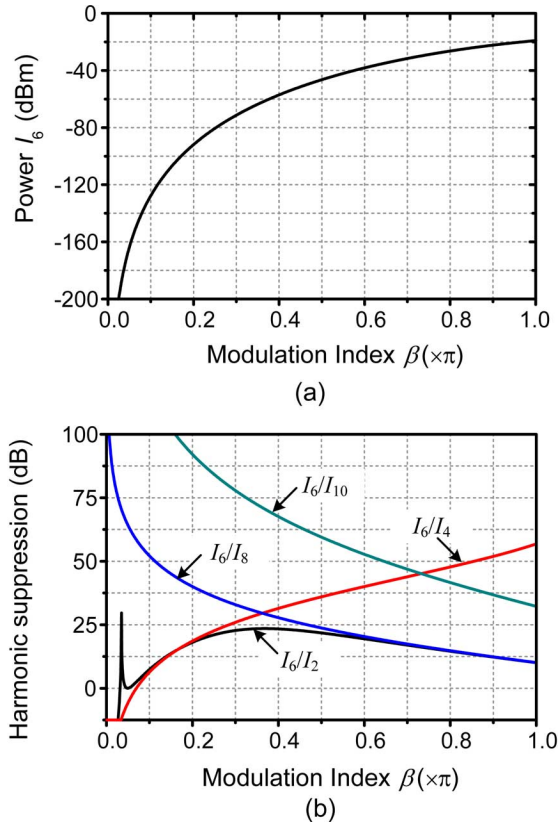

Fig. 3. Power and harmonic suppression ratios versus modulation index when $\alpha = 60$ dB. (a) Powers of the sixth-order harmonic I_6. (b) Harmonic suppression ratios $I_6/I_2, I_6/I_4, I_6/I_8$ and I_6/I_{10}.

From (9)–(13), we can see that $S_{\rm R}$ is dependent on the attenuation α of the optical notch filter and the phase-modulation index β. For a given α, a maximum value of $S_{\rm R}$ would be achieved by controlling β, which can be realized by adjusting the power of the microwave drive signal to the polarization modulator. Fig. 4 shows the maximum value of $S_{\rm R}$ and the corresponding β as a function of α. As can be seen, a larger attenuation α of the optical notch filter leads to a larger global suppression ratio. However, the corresponding phase-modulation index β is monotonically decreasing with α, showing a decreasing output power of the sixth-order electrical harmonic. This problem can be solved at a low cost by using an EDFA to increase the optical power before photodetection. It should be noted that a lower modulation depth corresponds to a less power requirement for the microwave drive signal [23].

III. Experiment

An experiment is performed based on the setup shown in Fig. 1(a). A light wave from a laser source is sent to the polarization modulator (Versawave Technologies) for complementary phase modulation. The polarization modulator is driven by a microwave signal from a microwave signal generator (Agilent E8254A). The phase modulation index is controlled to be approximately 0.46 π by setting the power of the microwave drive signal to be 18 dBm. The phase-modulated signals are converted to an intensity-modulated signal at a polarization beam splitter serving as the optical polarizer. A wavelength-fixed notch filter

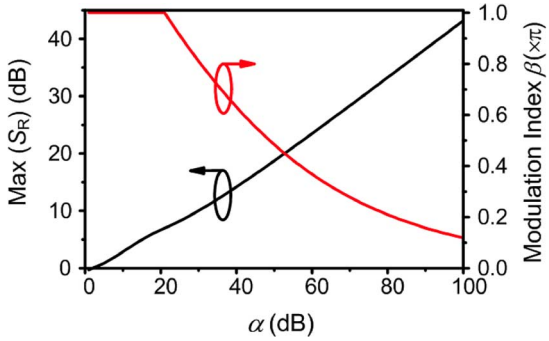

Fig. 4. Global suppression ratio and the corresponding β as a function of α.

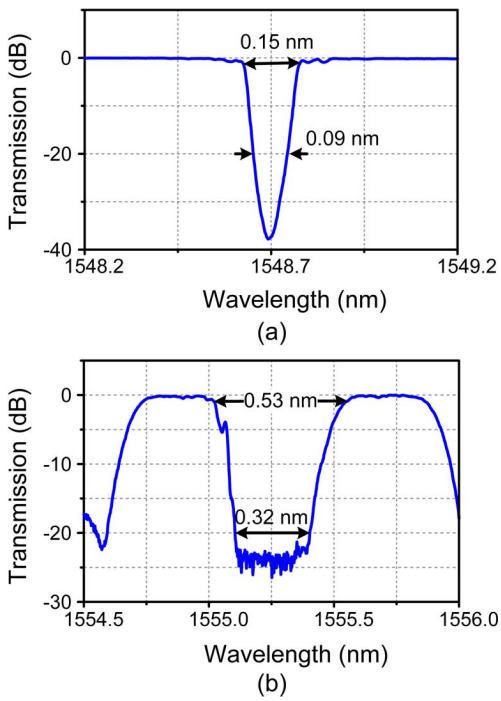

Fig. 5. Transmission spectra of two wavelength-fixed notch filters employed in the experiment.

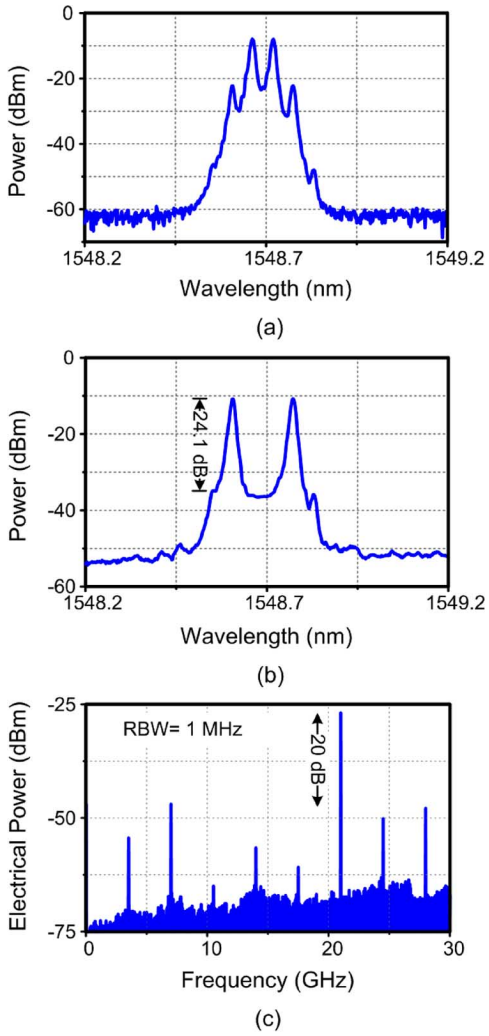

Fig. 6. Optical spectra (a) before the FBG filter and (b) after the FBG filter. (c) Electrical spectrum of the generated microwave signal.

is employed to suppress the undesired first-order sidebands. An EDFA is used to increase the power of the optical signal to a satisfactory level before photodetection at a 100-GHz uni-traveling carrier photodetector (u^2 t XPD4120R). The optical signal is monitored by an optical spectrum analyzer (Ando AQ 6317B) with a resolution of 0.01 nm, and the generated signal is observed by an electrical spectrum analyzer (Agilent E4448A, 3 Hz–50 GHz).

Since most of our measurement instruments only cover a frequency range from several megahertz to less than 50 GHz, we first investigate the performance of the frequency sextupler when it generates a microwave signal with a frequency less than 50 GHz. In this case, an FBG with its central wavelength (1548.73 nm) equal to the wavelength of the optical carrier is used as an optical notch filter, with the transmission spectrum shown in Fig. 5(a). The FBG is measured to have a bandwidth between the two minimum attenuation points of approximately 0.15 nm (∼18.75 GHz) and a bandwidth between the 20-dB attenuation points of approximately 0.09 nm (∼11.25 GHz). According to (5), the tuning range is about 18.75 ∼33.75 GHz. Due to the limited dynamic range of the optical spectrum analyzer, Fig. 5(b) only shows a rejection ratio at the central wavelength of about 36 dB. However, the actual rejection ratio should be much greater. In our measurement, we introduce a double-sideband signal into the filter. The carrier is 27 dB greater than the sidebands before the filter and is 34 dB lower than the sidebands after the filter, thus the rejection ratio should be over 60 dB.

Fig. 6(a) shows the optical spectrum at the output of the polarization beam splitter. The frequency of the electrical drive signal is set to be 3.5 GHz. Two first-order, two third-order, and two very weak fifth-order sidebands are observed. Excellent even-order sideband suppression is confirmed. The wavelengths of the two third-order sidebands are 1548.646 and 1548.814 nm, giving a wavelength spacing of 0.168 nm (21 GHz), which is six times the frequency of the electrical drive signal. With the two first-order sidebands removed by the FBG filter, the remaining two third-order sidebands are 24.1 dB higher than that of the optical carrier and other sidebands, as shown in Fig. 6(b). By applying the two wavelengths to the photodetector, a strong electrical signal with a frequency that is six times the frequency of

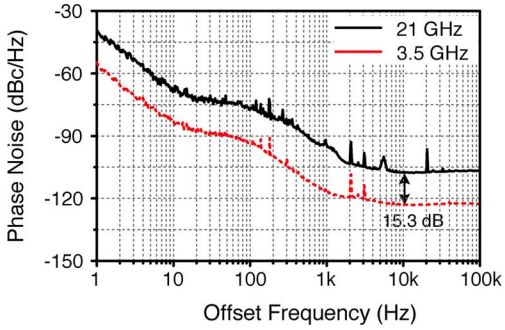

Fig. 7. Phase-noise spectra of the generated 21-GHz signal and the 3.5-GHz drive signal.

the electrical drive signal is observed, with the electrical spectrum shown in Fig. 6(c). Other harmonics in the electrical signal are also observed. As predicted in Fig. 3(b), the powers of I_2 and I_8 are greater than other undesirable harmonics. However, they are 20 dB lower than that of the frequency-sextupled component, which can be ignored for most of the applications. From the earlier analysis, a global suppression ratio of 20 dB requires at least 52-dB attenuation of the two first-order sidebands. Comparing Fig. 6(b) with Fig. 6(a), the two first-order sidebands are suppressed by 40 dB, which is much smaller than the actual value due to the limited dynamic range of the optical spectrum analyzer.

To investigate the spectral quality of the generated microwave signal, the phase noise of the signal is measured. Fig. 7 shows the single-sideband (SSB) phase noise spectrum of the generated 21-GHz signal measured by an Agilent E5052B signal source analyzer incorporating an Agilent E5053A down-converter. As a comparison, the phase noise spectrum of the 3.5-GHz microwave drive signal is also shown in Fig. 7. The phase noises of the 3.5- and 21-GHz signals are -122.82 and -107.57 dBc/Hz, respectively, at a 10-kHz offset frequency. The generated 21-GHz signal presents a 15.3-dB phase-noise degradation compared with the 3.5-GHz electrical drive signal. Theoretically, the phase noise of a frequency-sextupled signal should have a phase noise degradation of about $10\log_{10}6^2 = 15.56$ dB. The measurement is consistent with the theoretical prediction.

One of the key features of this technique is that no bias is needed for the polarization modulator, which makes the generated microwave signal have good power stability. To verify the conclusion, we allow the system to operate in a room environment for a period of 60 min with the optical and electrical spectra recorded at a 5-min interval. The results are shown in Fig. 8. As can be seen the amplitude variations of the 21-GHz component are small, which are within 0.4 dB. Since the 3.5-, 10.5-, 14-, and 17.5-GHz components are very small, they are more sensitive to the environmental variations. However, during the entire 60-min period, the $\sim$20 dB suppression ratio is always maintained.

The tunability of the generated microwave signal is also experimentally studied. When the frequency of the electrical drive signal is tuned from 3 to 4.6 GHz, a frequency-sextupled signal with a frequency tunable from 18 to 27.6 GHz is generated, as shown in Fig. 9. Because the optical notch filter used in the

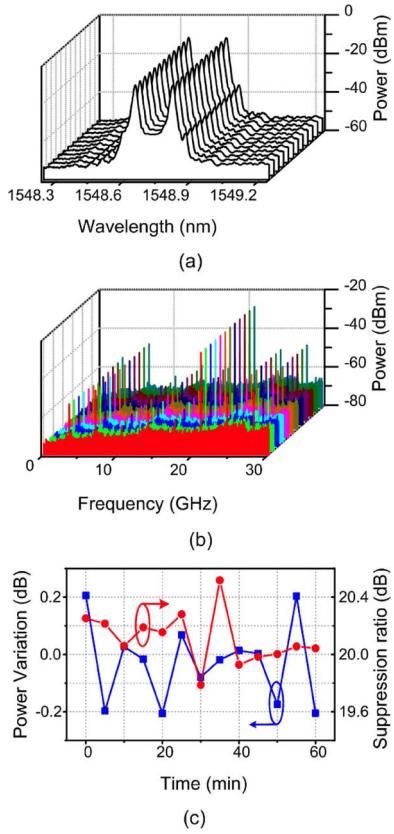

Fig. 8. Stability measurement of: (a) the optical spectra of the FBG filtered optical signal: (b) the electrical spectra of the generated electrical signal (RBW $=1$ MHz); and (c) power variations and suppression ratios at 5-min interval over a 60-min period.

experiment does not have an ideal isosceles-trapezoid-shaped transmission spectral profile as assumed in the analysis, the attenuation for the first-order sidebands at different frequencies will vary. As a result, the suppression ratio changes from 15.6 to 21.3 dB when the frequency of the microwave drive signal is tuned. Compared with the previously reported results for frequency-sextupled microwave signal generation [30], our method provides a better suppression ratio. It should be noted that only the frequency of the microwave drive signal is changed during the tuning process and other parameters are kept unaltered. If the phase-modulation index is also adjusted, as indicated in Fig. 4, the suppression ratio should be further improved.

To generate a subterahertz-wave signal using the proposed frequency sextupler, the FBG-based notch filter is replaced by an optical interleaver. From the transmission spectrum of the interleaver, as illustrated in Fig. 5(b), we can see that it has a bandwidth between the two minimum attenuation points of approximately 0.53 nm ($\sim$66 GHz) and a bandwidth between the 20-dB attenuation points of approximately 0.32 nm ($\sim$40 GHz). According to (5), the use of this interleaver would provide a frequency-tunable range of 66–120 GHz. Fig. 10 shows a typical optical spectrum of the filtered optical subterahertz-wave signal. As can be seen, the optical carrier and the two second-order sidebands are almost eliminated by carefully adjusting the polarization controller. The two third-order sidebands are 22 dB

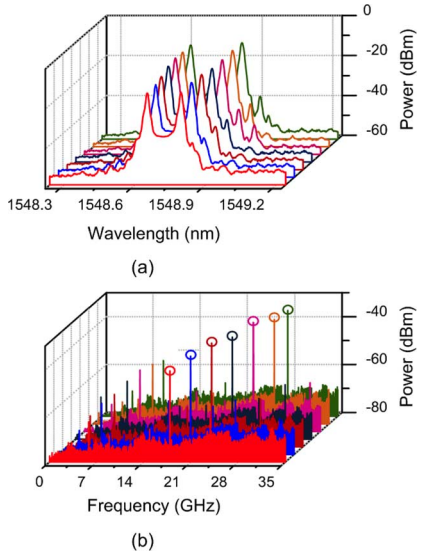

Fig. 9. Spectra of (a) the FBG filtered optical signal and (b) the generated electrical signal (RBW = 1 MHz) when the frequency of the electrical drive signal is tuned from 3 to 4.6 GHz.

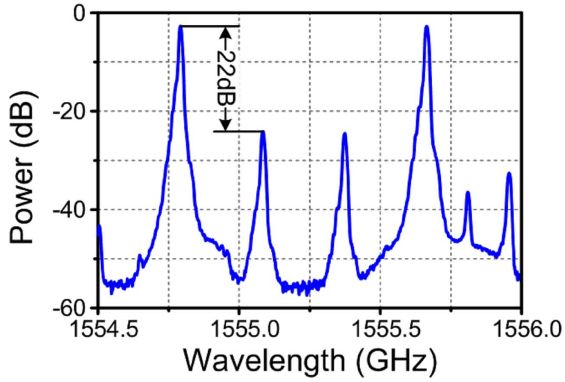

Fig. 10. Optical spectrum of the optical subterahertz wave signal at 108 GHz.

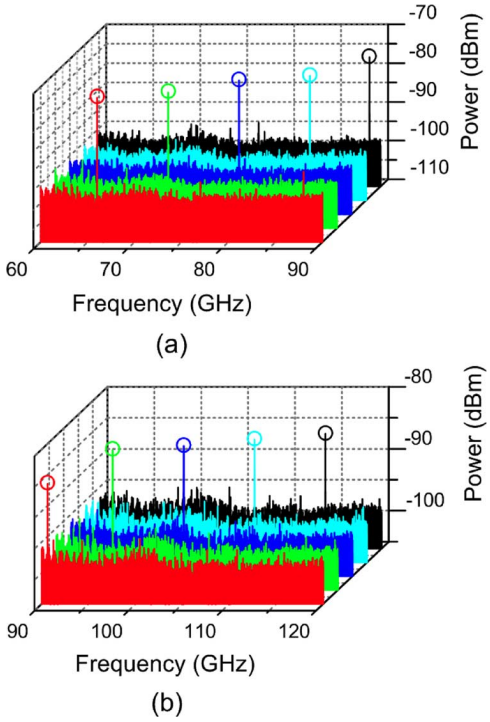

Fig. 11. Electrical spectra of the generated subterahertz wave at (a) 66–90 GHz and (b) 90-114 GHz when the frequency of the electrical drive signal is tuned from 11 to 19 GHz. RBW = 100 kHz.

higher than that of the first-order sidebands, indicating an effective suppression of the first-order sidebands by the optical interleaver. The wavelengths of the two third-order sidebands are 1554.794 and 1555.664 nm, giving a wavelength spacing of 0.87 nm (∼108 GHz), which is six times the frequency of the electrical drive signal (18 GHz). It should be noted that the fourth-order sidebands are observed from Fig. 10. This is because the polarization modulator is polarization-maintaining-fiber pigtailed. Mathematically, the influence of the differential group delay of the polarization-maintaining fiber on the signal generation performance can be considered by modifying (1) to yield

$$\begin{bmatrix} E_{\mathrm{x}}(t) \\ E_{\mathrm{y}}(t) \end{bmatrix} = \frac{\sqrt{2}}{2} \begin{bmatrix} \exp[j\omega_c t + j\beta \sin \omega_{\mathrm{m}} t] \\ \exp[j\omega_c (t+\Delta\tau) - j\beta \sin \omega_{\mathrm{m}} (t+\Delta\tau)] \end{bmatrix} \tag{15}$$

where $\Delta\tau$ is the differential group delay. Equation (2) is then changed to

$$\begin{aligned} E_{\mathrm{o1}}(t) = {} & 2\exp(j\omega_{\mathrm{c}} t) \cdot \sum_{n=1}^{\infty} J_{2n-1}(\beta) \\ & \cdot \{\sin[(2n-1)\omega_{\mathrm{m}} t] \\ & + \sin[(2n-1)\omega_{\mathrm{m}}(t+\Delta\tau)]t\} \\ & + \sum_{n=1}^{\infty} J_{2n}(\beta) \cdot \{\cos 2n\omega_{\mathrm{m}} t - \cos[2n\omega_{\mathrm{m}}(t+\Delta\tau)]\}. \end{aligned} \tag{16}$$

In obtaining (16), we assume that the fixed phase shift of $\omega_{\mathrm{c}}\Delta\tau$ is compensated by a wave plate or a polarization controller that is placed between the PolM and the polarizer. As can be seen from (15) and (16), the differential group delay introduces an additional phase shift between the signals along the two principal axes, which would deteriorate the suppression of the even-order sidebands when the two signals are combined at the polarizer. The amplitude of the $2n$th even-order sideband is written as $J_{2n}(\beta)\sqrt{2-2\cos(2n\omega_{\mathrm{m}}\Delta\tau)}$. In our demonstration, the differential group delay of the pigtailed polarization-maintaining fiber is about 0.35 ps, so it only degrades the suppression of the high-order sidebands. Practically, the polarization modulator and the polarizer would be integrated in a single monolithic chip, so the impact of the differential group delay on the system performance would be small and negligible, and thus the fourth-order sidebands should be fully eliminated.

To observe the 66–120-GHz subterahertz wave signal using the 3 Hz–50 GHz electrical spectrum analyzer, two external harmonic waveguide mixers (Tektronix WM782E 60-90 GHz and WM782F 90–140 GHz) are employed. Fig. 11 shows the spectra of the generated subterahertz-wave signal at different frequencies. When the frequency of the electrical drive signal is tuned from 11 to 19 GHz, the frequency of the generated frequency-sextupled signal varies from 66 to 114 GHz. Due to the

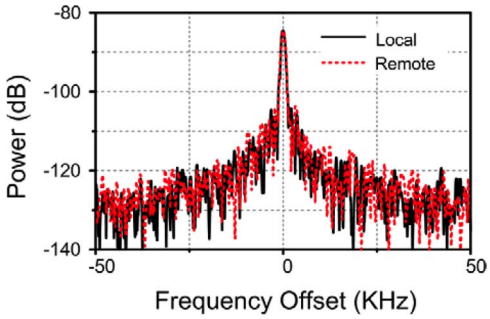

Fig. 12. Electrical spectra of the 114-GHz signal generated locally and remotely after transmission over a 40-km single-mode fiber. RBW = 91 Hz.

different conversion losses of the harmonic waveguide mixers, the powers of the subterahertz-wave signal in Fig. 11(a) are generally larger than that in Fig. 11(b). In the spectrum of the 66-GHz signal, a small 88-GHz component is also observed, but it is more than 19 dB lower than the 66-GHz component. Other spectra present only a single spectral line because the powers of the undesired beat signals are below the noise level.

To evaluate the quality of the generated electrical signal after fiber distribution, we transmit the optical subterahertz-wave signal over a 40-km standard single-mode fiber before photodetection. Fig. 12 gives the spectra of the 114-GHz signal generated locally and remotely. As can be seen, no obvious linewidth broadening is observed after fiber distribution, which indicates that the signal quality of the remotely generated signal is maintained. This feature is desirable for ultra-broadband wireless communications, where subterahertz-wave signals should be distributed to remote access points via optical fibers. It should be noted that an optical interleaver always have two complementary output; while one port outputs the two third-order sidebands, the other port outputs two first-order sidebands, which can be used to carry independent multiband services in a radio-over-fiber system [34].

IV. Conclusion

A novel method to implement microwave frequency sextupling using a polarization modulator and a wavelength-fixed optical notch filter was proposed and comprehensively studied. A theoretical analysis on the frequency tuning range and harmonic suppression ratio under different phase-modulation indices and filter attenuations were performed, with the analysis verified by a two-step experiment. In the first step, the frequency sextupler was operating at low-frequency regime, which allowed us to perform a comprehensive investigation of the performance of the proposed system using low-frequency measurement instruments. A narrow-bandwidth optical notch filter was employed in this step. A frequency-tunable microwave signal from 18 to 27.6 GHz was obtained by tuning the microwave drive signal from 3 to 4.6 GHz. The electrical harmonic suppression ratio was ∼20 dB. The phase-noise performance of the generated microwave signal was also evaluated. The phase noise of the generated signal was measured as low as −107.57 dBc/Hz at a 10-kHz offset frequency. The stability of the system was also investigated. In the second step, the narrow-bandwidth notch filter was replaced by an optical interleaver. A high-spectral-purity subterahertz-wave signal from 66 to 114 GHz was generated when the frequency of the drive signal was tuned from 11 to 19 GHz.

Compared with the previously reported optical frequency multiplication schemes based on an MZM, the proposed technique has three major advantages, which are: 1) the multiplication factor is six, which allows the generation of high-quality electrical signal with a frequency up to the subterahertz range using relatively low-frequency electrical and electrooptic devices; 2) the use of the polarization-modulator-based intensity modulator would provide a better performance in eliminating the even-order sidebands even if the frequency of the drive signal is high, so the spectral purity of the generated subterahertz wave could be significantly improved; and 3) no dc bias is needed for the polarization modulator, so the system is free from the bias drift, a serious problem when an MZM is biased at the minimum or maximum transmission point.

The proposed system also features a simple and compact structure, which can be used as a terahertz source for applications in spectroscopic sensing and ultra-broadband wireless communications.

References

[1] B. B. Hu and M. C. Nuss, "Imaging with terahertz waves," *Opt. Lett.*, vol. 20, no. 16, pp. 1716–, Aug. 15, 1995.
[2] Q. Wu, T. D. Hewitt, and X. C. Zhang, "Two-dimensional electro-optic imaging of THz beams," *Appl. Phys. Lett.*, vol. 69, no. 8, pp. 1026–1028, Aug. 19, 1996.
[3] W. L. Chan, J. Deibel, and D. M. Mittleman, "Imaging with terahertz radiation," *Rep. Prog. Phys.*, vol. 70, no. 8, pp. 1325–1379, Aug. 2007.
[4] A. Hirata, T. Kosugi, H. Takahashi, R. Yamaguchi, F. Nakajima, T. Furuta, H. Ito, H. Sugahara, Y. Sato, and T. Nagatsuma, "120-GHz-band millimeter-wave photonic wireless link for 10-Gb/s data transmission," *IEEE Trans. Microw. Theory Tech.*, vol. 54, no. 5, pp. 1937–1944, May 2006.
[5] J. Wells, "Faster than fiber: The future of multi-Gb/s wireless," *IEEE Microw. Mag.*, vol. 10, no. 3, pp. 104–112, May 2009.
[6] J. R. Demers, R. T. Logan, and E. R. Brown, "An optically integrated coherent frequency-domain THz spectrometer with signal-to- noise ratio up to 80 dB," in *Microw. Photon. Technol. Dig.*, Victoria, BC, Canada, Oct. 2007, pp. 92–95.
[7] T. Nagatsuma, "Generating millimeter and terahertz waves," *IEEE Microw. Mag.*, vol. 10, no. 4, pp. 64–74, Jun. 2009.
[8] X. F. Chen, J. P. Yao, and Z. Deng, "Ultranarrow dual-transmission-band fiber Bragg grating filter and its application in a dual-wavelength single-longitudinal-mode fiber ring laser," *Opt. Lett.*, vol. 30, no. 16, pp. 2068–2070, Aug. 15, 2005.
[9] S. L. Pan and J. P. Yao, "A wavelength-switchable single-longitudinal-mode dual-wavelength erbium-doped fiber laser for tunable microwave generation," *Opt. Exp.*, vol. 17, no. 7, pp. 5414–5419, Apr. 2009.
[10] S. L. Pan and J. P. Yao, "Frequency-switchable microwave generation based on a dual-wavelength single-longitudinal-mode fiber laser incorporating a high-finesse ring filter," *Opt. Exp.*, vol. 17, no. 14, pp. 12167–12173, Jul. 2009.
[11] L. Xia, P. Shum, and T. H. Cheng, "Photonic generation of microwave signals using a dual-transmission-band FBG filter with controllable wavelength spacing," *Appl. Phys. B, Lasers Opt.*, vol. 86, no. 1, pp. 61–64, Jan. 2007.
[12] M. Tani, P. Gu, M. Hyodo, K. Sakai, and T. Hidaka, "Generation of coherent terahertz radiation by photomixing of dual-mode lasers," *Opt. Quantum Electron.*, vol. 32, no. 4–5, pp. 503–520, May 2000.
[13] S. Hoffmann and M. R. Hofmann, "Generation of Terahertz radiation with two color semiconductor lasers," *Laser Photon. Rev.*, vol. 1, no. 1, pp. 44–56, Feb. 2007.
[14] Z. C. F. Fan and M. Dagenais, "Optical generation of a megahertz-linewidth microwave signal using semiconductor lasers and a discriminator-aided phase-locked loop," *IEEE Trans. Microw. Theory Tech.*, vol. 45, no. 8, pp. 1296–1300, Aug. 1997.

[15] L. N. Langley, M. D. Elkin, C. Edge, M. J. Wale, U. Gliese, X. Huang, and A. J. Seeds, "Packaged semiconductor laser optical phase-locked loop (OPLL) for photonic generation, processing and transmission of microwave signals," *IEEE Trans. Microw. Theory Tech.*, vol. 47, no. 7, pp. 1257–1264, Jul. 1999.
[16] M. Hyodo and M. Watanabe, "Optical generation of millimeter-wave signals up to 330 GHz by means of cascadingly phase locking three semiconductor lasers," *IEEE Photon. Technol. Lett.*, vol. 15, no. 3, pp. 458–460, Mar. 2003.
[17] A. Wiberg, P. Perez-Millan, M. V. Andres, and P. O. Hedekvist, "Microwave-photonic frequency multiplication utilizing optical four-wave mixing and fiber Bragg gratings," *J. Lightw. Technol.*, vol. 24, no. 1, pp. 329–334, Jan. 2006.
[18] Q. Wang, H. Rideout, F. Zeng, and J. P. Yao, "Millimeter-wave frequency tripling based on four-wave mixing in a semiconductor optical amplifier," *IEEE Photon. Technol. Lett.*, vol. 18, no. 24, pp. 2460–2462, Dec. 2006.
[19] T. L. Wang, H. W. Chen, M. H. Chen, J. Zhang, and S. H. Xie, "High-spectral-purity millimeter-wave signal optical generation," *J. Lightw. Technol.*, vol. 27, no. 12, pp. 2044–2051, Jun. 15, 2009.
[20] S. Fukushima, C. F. C. Silva, Y. Muramoto, and A. J. Seeds, "Opto-electronic millimeter-wave synthesis using an optical frequency comb generator, optically injection locked lasers, and a unitraveling-carrier photodiode," *J. Lightw. Technol.*, vol. 21, no. 12, pp. 3043–3051, Dec. 2003.
[21] M. Musha, A. Ueda, M. Horikoshi, K. Nakagawa, M. Ishiguro, K. Ueda, and H. Ito, "A highly stable mm-wave synthesizer realized by mixing two lasers locked to an optical frequency comb generator," *Opt. Commun.*, vol. 240, no. 1–3, pp. 201–208, Oct. 1, 2004.
[22] H. J. Song, N. Shimizu, T. Furuta, K. Suizu, H. Ito, and T. Nagatsuma, "Broadband-frequency-tunable sub-terahertz wave generation using an optical comb, AWGs, optical switches, and a uni-traveling carrier photodiode for spectroscopic applications," *J. Lightw. Technol.*, vol. 26, no. 15, pp. 2521–2530, Aug. 2008.
[23] G. Qi, J. P. Yao, J. Seregelyi, S. Paquet, and C. Bélisle, "Generation and distribution of a wideband continuously tunable millimeter-wave signal with an optical external modulation technique," *IEEE Trans. Microw. Theory Tech.*, vol. 53, no. 10, pp. 3090–3097, Oct. 2005.
[24] J. Zhang, H. W. Chen, M. H. Chen, T. L. Wang, and S. H. Xie, "A photonic microwave frequency quadrupler using two cascaded intensity modulators with repetitious optical carrier suppression," *IEEE Photon. Technol. Lett.*, vol. 19, no. 14, pp. 1057–1059, Jul. 2007.
[25] C. T. Lin, P. T. Shih, J. Chen, W. Q. Xue, P. C. Peng, and S. Chi, "Optical millimeter-wave signal generation using frequency quadrupling technique and no optical filtering," *IEEE Photon. Technol. Lett.*, vol. 20, no. 12, pp. 1027–1029, Jun. 2008.
[26] G. Qi, J. P. Yao, J. Seregelyi, S. Paquet, and C. Bélisle, "Optical generation and distribution of continuously tunable millimeter-wave signals using an optical phase modulator," *J. Lightw. Technol.*, vol. 23, no. 9, pp. 2687–2695, Sep. 2005.
[27] P. Shen, N. J. Gomes, P. A. Davies, W. P. Shillue, P. G. Huggard, and B. N. Ellison, "High-purity millimetre-wave photonic local oscillator generation and delivery," in *Proc. Int. Top. Meeting Microw. Photon.*, Sep. 10–12, 2003, pp. 189–192.
[28] S. L. Pan, C. L. Wang, and J. P. Yao, "Generation of a stable and frequency-tunable microwave signal using a polarization modulator and a wavelength-fixed notch filter," in *Proc. OFC*, 2009, paper JWA51.
[29] J. Zhang, H. W. Chen, M. H. Chen, T. L. Wang, and S. Z. Xie, "Photonic generation of a millimeter-wave signal based on sextuple-frequency multiplication," *Opt. Lett.*, vol. 32, no. 9, pp. 1020–1022, May 1, 2007.
[30] X. G. Chen, Z. L. Wang, and D. Chen, "Effects of direct current bias-drifting on radio on fiber link," *Int. J. Infrared Millim. Waves*, vol. 29, pp. 424–431, Apr. 2008.
[31] J. D. Bull, N. A. Jaeger, H. Kato, M. Fairburn, A. Reid, and P. Ghanipour, "40-GHz electro-optic polarization modulator for fiber optic communications systems," in *Proc. Photon. North 2004: Opt. Compon. Devices*, Ottawa, ON, Canada, 2004, pp. 133–143.
[32] C. C. Renaud, M. Robertson, D. Rogers, R. Firth, P. J. Cannard, R. Moore, and A. J. Seeds, "A high responsivity, broadband waveguide uni-travelling carrier photodiode," in *Millimeter-Wave and Terahertz Photon. Conf.*, Strasbourg, France, 2006, pp. 61940C–8.
[33] J. D. Bull, H. Kato, A. R. Reid, M. Fairburn, B. P. Tsou, D. R. Seniuk, P. H. Lu, and N. A. Jaeger, "Ultrahigh-speed polarization modulator," in *Proc. Conf. Lasers Electro-Opt./Quantum Electron. Laser Sci. Photon. Applic. Syst. Technol.*, 2005, paper JTuC54.
[34] Z. Jia, J. Yu, A. Chowdhury, G. Ellinas, and G. Chang, "Simultaneous generation of independent wired and wireless services using a single modulator in millimeter-wave-band radio-over-fiber systems," *IEEE Photon. Technol. Lett.*, vol. 19, no. 20, pp. 1691–1693, Oct. 2007.

Shilong Pan (S'06–M'09) received the B.S. and Ph.D. degrees in electronics engineering from Tsinghua University, Beijing, China, in 2004 and 2008, respectively.

In August 2008, he joined the Microwave Photonics Research Laboratory, School of information Technology and Engineering, University of Ottawa, Ottawa, ON, Canada, as a Postdoctoral Research Fellow. His current research interests include ultra-wideband over fiber, ultrafast optical signal processing, fiber lasers, and terahertz wave generation.

Dr. Pan is a member of the Optical Society of America and the IEEE Photonics Society.

Jianping Yao (M'99–SM'01) received the Ph.D. degree in electrical engineering from the Université de Toulon, Toulon, France, in 1997.

He joined the School of Information Technology and Engineering, University of Ottawa, Ottawa, ON, Canada, in 2001, where he is currently a Professor, Director of the Microwave Photonics Research Laboratory, and Director of the Ottawa—Carleton Institute for Electrical and Computer Engineering. From 1999 to 2001, he held a faculty position with the School of Electrical and Electronic Engineering, Nanyang Technological University, Singapore. He holds a Yongqian Endowed Visiting Chair Professorship with Zhejiang University, China. He spent three months as an Invited Professor with the Institut National Polytechnique de Grenoble, Grenoble, France, in 2005. He has authored or coauthored over 270 papers including 150 papers in peer-reviewed journals and over120 papers in conference proceeding. His research has focused on microwave photonics, which includes all-optical microwave signal processing, photonic generation of microwave, millimeter-wave, and terahertz, radio over fiber, ultra-wideband over fiber, fiber Bragg gratings for microwave photonics applications, and optically controlled phased array antenna. He is an Associate Editor of the *International Journal of Microwave and Optical Technology*. His research interests also include fiber lasers, fiber-optic sensors and bio-photonics.

Dr. Yao is a Registered Professional Engineer in the Province of Ontario. He is a Fellow of the Optical Society of America (OSA) and a Senior Member of the IEEE Photonics Society and the IEEE Microwave Theory and Techniques Society. He is on the Editorial Board of the IEEE TRANSACTIONS ON MICROWAVE THEORY AND TECHNIQUES. He was the recipient of the 2005 International Creative Research Award of the University of Ottawa and the 2007 George S. Glinski Award for Excellence in Research. He was named University Research Chair in Microwave Photonics in 2007. He was the recipient of a Natural Sciences and Engineering Research Council of Canada (NSERC) Discovery Accelerator Supplements Award in 2008.